APPROVED:

Leonid N. Litvinenko,

**Institute Director** 

# Project Report HF/VHF Radar Backscatter by Artificial Small-Scale

Ionospheric Turbulence

(EOARD Special Contract F6170896W0321)

DISTRIBUTION STATEMENT

Approved for public release; Distribution Unlimited Principal Investigator:

Yuri M. Yampolski,

Laboratory Leader

DITTO QUALITIES RECEIPTED 3

Institute of Radio Astronomy Kharkov, Ukraine

December, 1997

19980423 031

Public reporting burden for this collection of info gathering and maintaining the data needed, and collection of information, including suggestions Davis Highway, Suite 1204, Arlington, VA 22202	d completing and reviewing the collection of in for reducing this burden to Washington Head 2-4302, and to the Office of Management and I	nformation. Send comments regard equarters Services, Directorate for Budget, Paperwork Reduction Proj	ding this burden estimate Information Operations ar ect (0704-0188), Washingto	or any other aspect of this d Reports, 1215 Jefferson			
AGENCY USE ONLY (Leave blank)	2. REPORT DATE		RT TYPE AND DATES COVERED				
	December 1997		Final Report				
4. TITLE AND SUBTITLE	1		5. FUNDING NUMBE	RS			
HF/VHF Radar Backscatter by	F6170896W0321						
6. AUTHOR(S)							
Dr. Yuri Yampolski							
7. PERFORMING ORGANIZATION NAME	8. PERFORMING ORGANIZATION REPORT NUMBER						
Institute of Radio Astronomy ( 4, Chervonopraporna Str Kharkov 310002 Ukraine	N/A						
9. SPONSORING/MONITORING AGEN	10. SPONSORING/MONITORING AGENCY REPORT NUMBER						
EOARD BOY 44							
PSC 802 BOX 14 FPO 09499-0200	SPC 96-4100						
11. SUPPLEMENTARY NOTES							
12a. DISTRIBUTION/AVAILABILITY STA	ATEMENT	•	12b. DISTRIBUTION CODE				
Approved for public release; d	A						
13. ABSTRACT (Maximum 200 words)							
This report results from a contract tasking Institute of Radio Astronomy (RIAN) as follows: The contractor shall carry out a program of study of artificial small-scale turbulence (ASST) generated in the ionosphere by the high-power transmitter operated by the Radiophysical Research Institute at Nizhny Novgorod, Russia. A primary goal of the investigations will be to determine how the various processes are affected by changes in the exciting source field of the high-power HF wave.							
14. SUBJECT TERMS	THE RESIDENCE OF THE PARTY OF T		15. NUN	MBER OF PAGES			
Geophysics			16. PRICI	29 E CODE N/A			
17. SECURITY CLASSIFICATION OF REPORT	18. SECURITY CLASSIFICATION OF THIS PAGE	19, SECURITY CLASSIFICA OF ABSTRACT	TION 20. LIMIT	ATION OF ABSTRACT			

REPORT DOCUMENTATION PAGE

UNCLASSIFIED

UNCLASSIFIED

UNCLASSIFIED

Form Approved OMB No. 0704-0188

#### Introduction

The decameter wavelength bistatic radar that was jointly developed in 1995 by groups of researchers from the Institute of Radio Astronomy and the University of Kharkov for investigating the time and space structure of stimulated ionospheric turbulence (SIT) consisted of a transmitting system and a receiving complex separated in space. The measurements that were carried out in the pulsed and CW modes and the rich variety of results obtained demonstrated the high working capacity of the radar and its conformance to the initially set specifications [1]. Meanwhile, the parallel CW measurements with the use of radiation from HF broadcasting stations and special transmitters of the Time and Frequency Service have shown the possibility of obtaining extra information by simultaneously employing several radio frequencies. That could be, for instance, the information on the line-of-sight velocity component of ionospheric inhomogeneities of different scale sizes taken at the same time moment. Besides, operation of the radar itself revealed some of its technical limitations. For these reasons, the first model of the radar was subjected to essential upgrading as part of preparations for the US-Ukrainian measuring campaign initially planned for September, 1997. The principal aim was to develop a dual-frequency bistatic HF radar for ionospheric research. This Report contains a detailed description of the modernized radar complex and presents some of the results obtained during a test campaign.

# 1. Up-grade of the Transmit-Receive Complex and Data Acquisition and Data Processing System

# 1.1. Up-grade of the Transmitter

The transmitter system of the prior radar involved a pulsed transmitter generating square-wave radio pulses of a 30 to 100  $\mu$ s duration at carrier frequencies between 3 and 20 MHz, and a phased array antenna (PA) radiating effectively at 14.5 to 33 MHz. The up-grade concerned both the transmitter and the antenna. First, the operating range of the transmitter was extended to the higher frequency end up to 26 MHz. The triggering circuits were essentially modified. While initially the transmitter allowed operation at a single frequency, the up-graded unit can generate pulses at two frequencies from the operating range simultaneously. In this case the first and all odd-numbered pulses to follow have the filling frequency  $f_1$ , whereas all even-numbered pulses are at  $f_2$ . Each of the frequencies  $f_1$  and  $f_2$  is provided by its own synthesizer adjustable in discrete steps of 0.01 Hz. Having in mind the required accuracy of Doppler shift measurements of the radar echoes (to restore the line-of-sight velocity component of ionospheric inhomogeneities), the two synthesizers are fed from the same master oscillator characterized by the long-term (24 hours) relative instability of  $2x10^{-8}$  and short-term instability about  $10^{-9}$ .

To improve the antenna performance, the matching units and the r.f. cable connecting the PA to the transmitter were replaced. As a result, ohmic losses in the system have been reduced and the traveling wave ratio increased from 0.6 or 0.8 to 0.8 or 0.95 through the operation range. Accordingly, the average radiated power has somewhat increased. While the former highest repetition frequency was 25 Hz for pulses of 100 µs duration, now the value can reach 40 Hz. The

increase in the pulsed and average radiated power should allow improving the signal-to-noise ratio at the receive end of the radar, both for measurements of spatial parameters and frequency characteristics of the echoes.

With all the improvements, the up-graded transmitter system of the radar is characterized by the performance parameters as follows

- operating frequency range 14.5 to 26 MHz with the traveling wave ratio 0.8 to 0.95;
- pulsed radiated power 70 to 100 kW
- average radiated power 300 to 400 W (the corresponding highest repetition frequency is 40 Hz with 100 μs pulses at a single carrier or 20 Hz at either of two carrier frequencies);
- directivity factor of the antenna about 20 at mid-point of the operating range.

# 1.2. Up-grade of the Receive Complex

The receive complex has been up-graded to match the concept of a dual-frequency bistatic radar. The former set of data acquisition equipment allowed for parallel reception and digitization of two pulsed signals of up to 10 kHz bandwidths. The new complex accommodates four identical analog channels. Each of the channels involves a selection filter (SF) with a bell-like response function, providing for a matched transmission of signals within the 10 kHz band and suppression off the band. At the same time, the SFs employed are characterized by a smooth amplitude-vs-frequency response without oscillations or steep edges (unlike quartz based or electromechanical filters). Therefore, these filters do not produce characteristic surges of the input voltage when fed with a broadband (pulsed) signal. Such surges might seriously impede interpretation of the radar echoes. The up-graded data acquisition and data processing complex incorporates four channels to receive pulsed signals, which allows parallel reception in four pattern beams of the UTR-2 radio telescope employed as the radar receive antenna. (The reception pattern of the telescope's North-South arm represents five spatially separated beams, with yet another beam being formed by the East-West arm.) In the case of parallel operation on two frequencies, reception can be performed in two beams at each frequency, with the beams not necessarily the same.

A different four-channel coherent configuration can be realized in the single-frequency pulsed mode. Then the receiver input will take the signals from three beams of the N-S array and the one E-W. By scanning the beams, this configuration implements a 3D radar with a high Doppler resolution.

The analog equipment used to receive narrow-band (CW) signals has not been modified and provides, as before, six independent reception channels of 20 Hz widths. Each channel can be connected to any beam of the array pattern and adjusted (to discrete steps of 0.01 Hz) to any frequency from the operating range.

# 1.3. Data Acquisition and Data Processing System

As stipulated by the Contract, works of the first stage were centered on up-grading the radar equipment for data acquisition, processing and storage, with the aim of increasing the rates and reliabil-

ity of data reading / writing, visualization and archiving. To speed up the processes, the system was modified along two lines. First, efforts were made to purchase and install fast hardware and, second, to improve the software. The equipment purchased included an ADC much faster than before, a PC and a CD recorder. In what follows, the specifications of the newly acquired equipment are compared with the previous parameters.

- a) ADC. The 12-bit, 16-channel CIO-DAS16F converter that was used in prior measuring campaigns was characterized by a maximum pick-up frequency of analog data equal to 50 kHz. With a 10 kHz bandwidth of the sounding pulse that provided for simultaneous operation of only two radar channels. The new ADC, L-1250, is also capable of providing a 72 dB dynamic range (12 bit), however shows a much higher digitization rate (specifically, 500 kHz, or a 1.8 µs conversion time). It should be noted that the actual rate is somewhat lower (the corresponding frequency is 300 to 330 kHz), being limited by the throughput of the PCI bus used for data transfer. However, it is more than sufficient for digitizing the input from the current four channels (the required frequency is 20.4=80 kHz). Other conveniences provided by the L-1250 card are the built-in signal processor ADSP-2105 and the internal FIFO buffer to accommodate 8 K words. These allow reducing the load on the central processor. The ADC operation threshold can be regulated, depending on the input signal level, owing to availability of a front-end amplifier with a program-selectable amplification factor (1, 2 or 4 for the input voltages of 5.12 V; 2.56 and 1.024 V, respectively). This can be regarded as an equivalent 12 dB extension of the dynamic range. The number of analog channels also has been increased to become 16 differential or 32 commonearth channels. The former 16-channel ADC and the corresponding software are used in the new acquisition system for digitizing low-frequency quasi-monochromatic signals, thus bringing all data records to a unique format.
- b) PC. To allow real time acquisition and processing of the data, a Pentium computer has been installed. The 64-bit arithmetic, 200 MHz clock frequency and the powerful video card pertinent to the computer have allowed to greatly increase the speed of data pick-up, processing and display as compared with the former computer (80486 DX-2 processor and 66 MHz clock frequency). A quick-access hard disk SCSI-4 of 2.1 GB capacity has been installed instead of the 1.05 GB SCSI-2. As a result, continuous data recording during 3 hours and 40 minutes is possible in four pulsed radar channels. The stored data can be retrospectively processed over a considerably shorter time than before, owing to the increased memory capacity (64 MB instead of 16 MB). In fact, the problem with pulsed signals processing stems from the necessity of repeatedly reading the same data carrying sections of the file. If these sections are temporarily stored in the main memory, then the access is facilitated and wear of the hard disk avoided.
- c) CD recorder. To ensure long term storage of the data, the prior system used an EXB-8505 tape drive. The advantage of that archive was its ability to store large arrays of data in the same physical carrier (the capacity of one magnetic tape varies between 5 and 20 GB, depending on the compression ratio). The inconvenience of the tape drive is its low access rate arising from the inherently serial mode of operation. In addition, the experience gained during prior measuring campaigns revealed an extremely poor reliability of the drive itself and the software. For these reasons, the device has been replaced by a writing CD drive. Test measurements in the fall of 1997 showed the drive to be a reliable and convenient device. The capacity of a single CD is 650 MB, which is sufficient for recording the

data of a one-hour session of measurements in four pulsed channels. Besides, the CD drive is a parallel-access device providing a high rate of data exchange (comparable with that of a computer hard disk).

Software modifications mainly concerned adaptation of the former applied package to both varieties of the hardware available, i.e. L-1250 and CIO-DAS16F. The program has also been complemented by a timing unit to ensure that the ADC of both the pulsed and the CW channel could be triggered by signals from a GPS receiver. The data to be processed can be stored temporarily in the main memory (see item b), which results in a factor 7 to 10 reduction of the time required for data retrieval and analysis. The potential for processed data presentation has been considerably increased by introduction of new subprograms to compute and display new spatial parameters of the objects under investigation, e.g. effective width and asymmetry of the modified area in the ionosphere. High quality color hard copies of the graphic displays have become possible through purchase and installation of the EP-SON Stylus color printer. The general structure of the data processing system is given in Fig. 1.

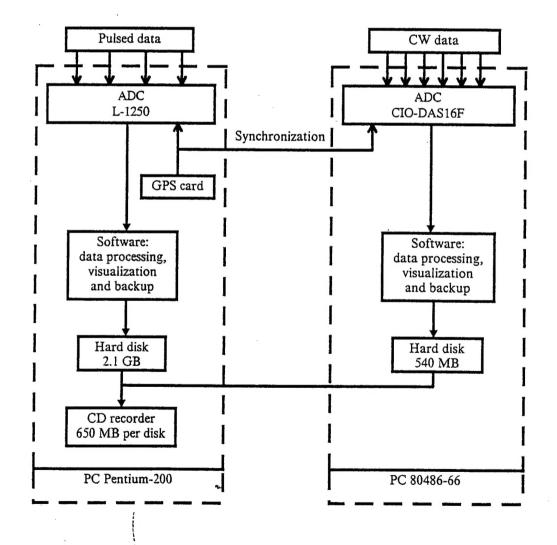


Fig. 1. Functional diagram of the data acquisition and data processing system.

# 2. Trial Measuring Campaign

# 2.1. Geometry and Configuration of the Experiment

The trial measuring campaign aimed at testing the up-graded hardware and the data taking system was held October 21 through 25, 1997. The working hours were 13:30 to 17:30, local time, with the total net duration of the experiment close to 20 hours. The radio facilities employed included

- i) the experimental bistatic radar. The transmit site was located at 49.63 deg N and 36.33 deg E, and the receive site at 49.67 deg N and 36.83 deg E.
  - ii) the powerful "heating" transmitter Sura at 56.22 deg N and 46.17 deg E.
- iii) radio RWM (transmitter of the Russian Time and Frequency Service [2]) 55.8 deg N and 38.3 deg E.
  - iv) a CW diagnostic transmitter located near Novocherkassk, Russia.

In addition, fluctuations in the geomagnetic field were measured with a high sensitivity magnetometer in a close vicinity of the radar receive site.

The locations of all the measuring sites are shown in the map of Fig.2.

The radar echoes were observed and recorded as follows.

The ionospheric plasma was modified by the radiation from the Sura "heater" at a frequency somewhat lower than  $f_{0F2}$ . (Both vertically and obliquely incident radiation was used). In most cases the powerful radiation was emitted in pulses of 3 to 5 min duration and duty factor about 1. Details of the operation schedule are given in the companion Report by NIRFI, Nizhny Novgorod.

The diagnostic radar was emitting pulsed signals continuously during 4 hours, simultaneously at two frequencies close to 19 and 21 MHz. Precise frequencies were selected depending on the noise environment at the receive site and occasionally were varied, following a command from the receive site. The duration of the sounding pulse was 100 µs and the repetition frequency 15 Hz at each of the carriers. The pulsed radiated power was close to 90 kW.

At the same time, the other diagnostic transmitter (located near Novocherkassk) radiated CW signals at 23.725 MHz. The power was close to 5 kW.

The Time Service radio operated in its periodic mode, i.e. 8 minutes of CW radiation were followed by a one minute break, then one minute of call signing and 20 minutes of pulsed radiation. Specifically, the latter included 10 minutes of pulses with a 1 Hz repetition frequency and 10 minutes with that of 10 Hz. After that, the next cycle followed.

The broadband (pulsed) channels at the receive end were adjusted pair-wise to the frequencies radiated by the radar transmitter. Over the periods when the "heating" transmitter was on, the outputs of the pulsed channels were digitized and recorded. In addition, the broadband signals were displayed in the analog form. If an echo was detected visually at one of the operating frequencies while absent at the other, then all the pulsed channels were switched to the same "active" frequency. In this case the echoes from the artificially stimulated ionospheric turbulence were received through a greater number of the antenna beams, thus carrying more information on the spatial structure of the scattering domain.





Fig. 2. Experimental lay-out.

The six narrow band channels were split into two equal groups. Group 1 channels were tuned to the operating frequency of Radio RWM (i.e. either 14.996 MHz or 9.996 MHz, depending on the current electron density profile), while group 2 to the second diagnostic frequency of 23.725 MHz. The outputs of all the six channels were digitized and recorded. The signals in each channel were also used to compute their Fourier spectra in real time, with the result displayed. If an echo was observed at one of the operating frequencies but absent at the other during an "active" period of the Sura transmitter (heater on), then most of the narrow band channels were tuned to that frequency. Similar as with the pulsed mode, this allowed collecting more information on the scattering area.

During some of the experiments a narrow band channel was tuned to the operating frequency of the "heating" transmitter, Sura.

In some measurements the reception pattern of the UTR-2 array was scanned over angles. The beam orientation was changed according to a special program over the length of one heating pulse.

The results will be presented and discussed in the appropriate section of this Report.

The radar observations were accompanied by ground-based magnetic measurements. The techniques and results will be discussed bellow.

#### 2.2. CW Mode

As noted earlier, the area of stimulated ionospheric turbulence was sounded both in the pulsed and CW mode. While providing ample information on the "heated" region, the pulsed mode, if applied continuously, required greater memory resources and was inconveniently inertial with regard to "through" processing of the complete set of observational data. In contrast to that, the CW mode did not require operation of a special-purpose transmitter, could be easily implemented continuously and was accessible to operational scanning of the results. In addition, the high directional properties of the UTR-2 array antenna, combined with the six-frequency channels of the receive complex, partially compensated the lack of range resolution. The elevation angle resolution was achievable owing to the multibeam pattern, while azimuth resolution resulted from scanning. Therefore, CW signals were recorded continuously through the entire daily work cycle of the heating facility. This allowed real-time monitoring of the area of artificial turbulence and suggested optimum moments for switching the pulsed mode on.

The diagnostic radiation that was used to investigate the ionospheric turbulence in the CW mode came from radio facilities, specifically Radio RWM ( $f_1 = 9.996$  MHz and  $f_2 = 14.996$  MHz), and a dedicated HF transmitter near Novocherkassk (f = 23.725 MHz). The total duration of records accumulated over the measuring campaign is 20 hours. Two methods of observation were employed: i) a fixed reception pattern oriented toward the assumed location of the artificial turbulence, and ii) angular scanning of the pattern. While the first method was used in many prior campaigns, the second one has been tested now for the first time.

Consider the scanning technique in more detail as it allowed representing the modified ionospheric region visually in the elevation angle - azimuth coordinates. The elevation angle distribution of the scattered diagnostic intensity was computed through cross-correlation analysis of the signals received in the five pattern beams of the N-S array and one E-W beam. This has proven possible because the intersection areas of the E-W beam oriented toward the heated region with the five "knife-edge" beams of the N-S array were spaced in the elevation angle but not in the azimuth. The azimuthal dependence could be analyzed, in principle, by scanning the multibeam pattern.

Table 1

Date	Time (UT)	Range of azimuth angles	Step in azi- muth	Elevation angle of the central beam (N-S)	Sounding frequency (MHz)
10/22/97	11:37-11:40	30°- 40°	2°	20°	23.725
10/22/97	12:01-12:04	30°- 40°	2°	20°	14.996
10/22/97	12:25-12:28	32°- 42°	2°	20°	14.996
10/22/97	12:31-12:34	32°- 42°	2°	20°	14.996
10/22/97	12:43-12:46	32°- 42°	2°	20°	14.996
10/24/97	13:31-13:34	29°- 44°	3°	20°	14.996
10/24/97	13:43-13:46	29°- 44°	3°	20°	14.996
10/24/97	13:55-13:58	29°- 44°	3° .	20°	14.996
10/25/97	13:01-13:06	27°- 45°	2°	20°	14.996

Nine scanning sessions were performed in the campaign. The periods selected for scanning were characterized by steady state operation of the Sura transmitter when neither the radiated power, nor frequency were varied. Specific parameters of the scans are listed in Table 1. The data have been used to compute the scattered intensity distributions of the diagnostic radiation in the azimuth-elevation angle coordinates. A typical example is given in Fig. 3A, where the elevation angle is along the vertical axis, the azimuth along the abscissa and the normalized scattered intensity is represented in false colors. As can be seen, the maximum scattered intensity is near 38° in azimuth and 20.5° in the elevation angle, and the area occupied by stimulated turbulence is of ellipsoidal geometry. However, in some cases the angular dependence of the scattered intensity was more complex. Fig. 3B shows the angular portrait of an area consisting of two components separated along the elevation. This splitting of the turbulent area into two subregions was fixed in all the three scanning sessions of 24 October, 1997.

When operated with a fixed orientation of the reception pattern, the receive complex used the configurations as follows:

- 1) The reception channels were connected to different pattern beams (i.e. N-S 1; N-S 2; N-S 3; N-S 4; N-S 5 and E-W) but tuned to the frequency of the same diagnostic source. This configuration allowed comparing the dynamics of scatterer motions and decay rates of the inhomogeneities for separated parts of the scattering volume.
- 2) The reception channels were adjusted to operating frequencies of several transmitters. In certain cases the "heating" frequency was recorded along with the diagnostic emissions. This configuration was used to compare scattered intensities of the diagnostic signals at different frequencies (9.996 MHz; 14.996 MHz and 23.725 MHz) coming from different sources (i.e. transmitters near Moscow or Novocherkassk). The results of preliminary processing indicate the scattered amplitude of the Novocherkassk

source to be normally lower than of the Moscow transmitter. The difference was particularly great during local day (see Fig. 4A), while in the evening the scattered signal from Novocherkassk increased (Fig. 4B).

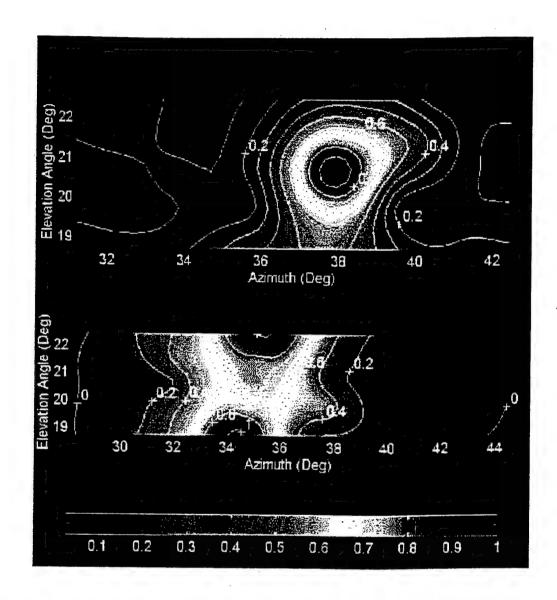


Fig. 3. Scattered intensity distributions of the diagnostic radiation in the azimuth-elevation angle coordinates.

Among the physical effects of interest that were detected in the 1997 campaign one was observation of quasiperiodic Doppler shift variations about 10 Hz in amplitude and a quasiperiod of a few minutes (Fig. 5). Normally, the Doppler frequency shift of scattered diagnostic signals remains within one or two hertz.

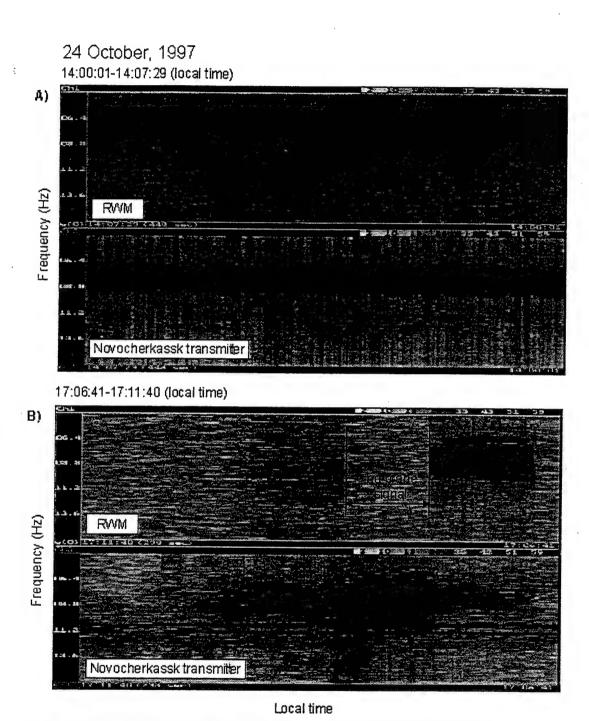


Fig. 4. Diagnostic signal specgrams from Radio RWM and the Novocherkassk transmitter.

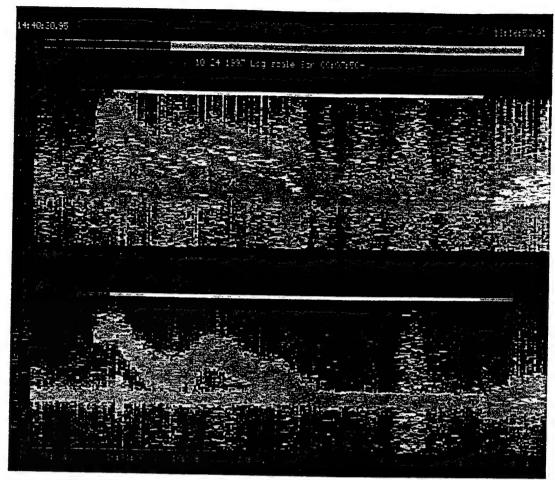


Fig. 5. Giant Doppler shift variations.

# 2.3. Pulsed Mode

The integrated duration of measurements in the pulsed mode of the diagnostic bistatic radar is 7 hours. The signals from the special research transmitter located at the Radio Physical Observatory (RPO) of the University of Kharkov were recorded 22 through 24 October, 1997. October 21 the transmitter was inoperative because of interrupted power supply at RPO. October 25 the transmitter was active during the entire measuring period, however the signal was not detected at the receive site owing to highly disturbed ionospheric conditions (a powerful sporadic E layer was present). The dates of 21 and 24 October were used for calibrations and for recording the pulsed signals of Radio RWM with a 10 Hz repetition frequency (emitted between minutes 20 and 30, and minutes 50 and 60 of each hour). The trial campaign has confirmed the operation capacity of the up-graded data acquisition / data processing system and revealed some of its defects which it would be desirable to eliminate before the start of the full scale measuring campaign. One of the drawbacks is the timing problem at the receive site impeding absolute range measurements. The problem arises from the extremely low level of the ground wave from the RPO transmitter, which is a result of the up-grade effort, hence improved matching in the transmitter-antenna cable.

Consider the observational facts found in the campaign. With a properly selected sounding frequency, the radar permitted reliable detection of the scattered signals and determination of the intensity-vs-range dependence. Shown in Fig. 6 is the time-space map of the modified ionospheric region

taken 23 October (the ranges along the vertical should be regarded as relative rather than absolute values). The heating facility was operated in the "40 sec on - 80 sec off" regime. The range to the "heated" area can be seen to have varied by about 150 km, which seems to be a new effect. Similar behavior of the turbulent region was noted on October 24 too (Fig. 7). On that date the powerful transmitter admittedly was operated in a three-minute cycle (1 min on - 2 min off), however the figure shows no signs of decay of the stimulated inhomogeneities.

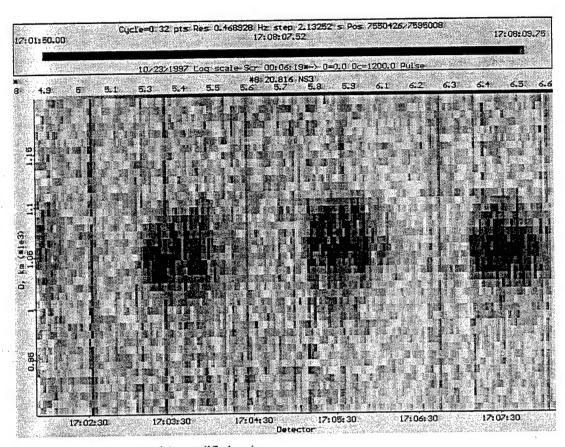


Fig. 6. A time-range map of the modified region.

Like in prior campaigns, the echoes of pulsed diagnostic signals showed quasiperiodic variations of the Doppler frequency shift over the periods of sufficiently high geomagnetic pulsations. An example is shown in Fig. 8. The Doppler velocity variations were observed at a distance of 997.5 km. Fig. 9 shows a pair of brightness images of the "heated" region in the range-frequency frame, with the second image in the pair obtained some 2.5 minutes after the first. As can be seen, the modified region is involved in quasiperiodic motion as a whole, with invariant width of the scattered spectrum. The mean value of the Doppler frequency shift is -1.5 Hz in Fig. 9A and -2.5 Hz in Fig. 9B.

A sharply different case (in fact, observed for the first time) is shown in Fig. 10. Once again, the figure presents time-and-space maps of the "heated" region, taken at several consecutive time moments. It seems obvious that the frequency variations do not occur synchronously at different ranges. That can be also seen from Fig. 11 representing frequency / time "snapshots" of the scattering volume taken from two different locations that were separated by 450 km. Note that the size of the turbulent region as was observed was conditioned by the special operation mode of the heating facility, where the radiation pattern of the powerful transmit antenna consisted of two identical lobes separated by some 6 to 12 degrees within the meridional plane.

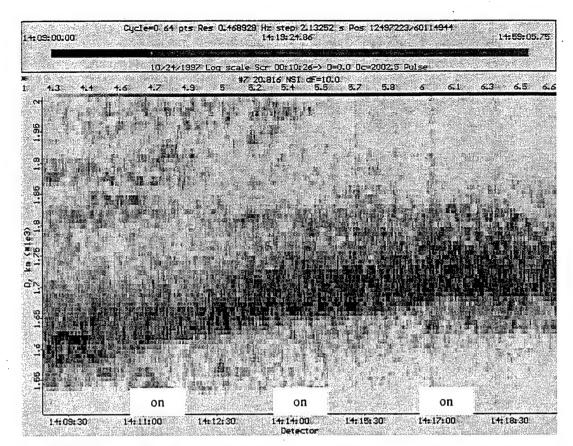


Fig. 7. Drift of the turbulized area.

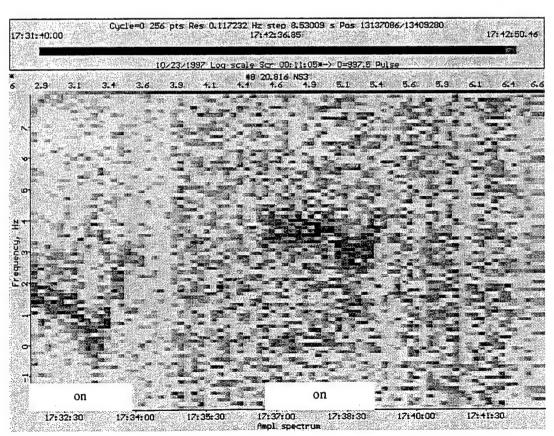
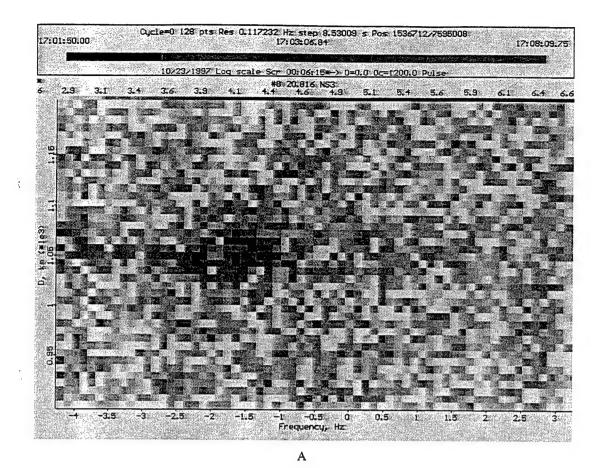


Fig. 8. Quasiperiodic variations in the Doppler frequency shift.



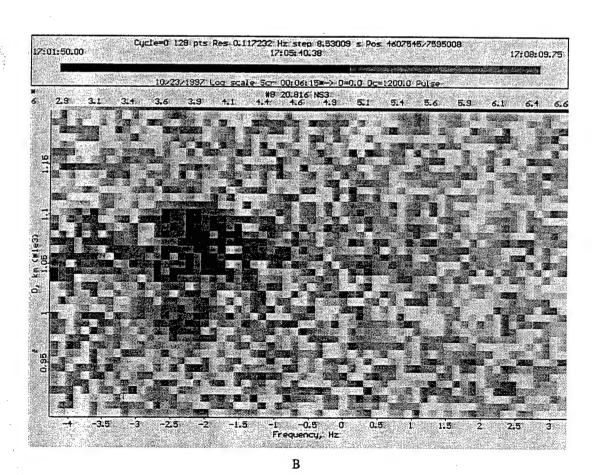
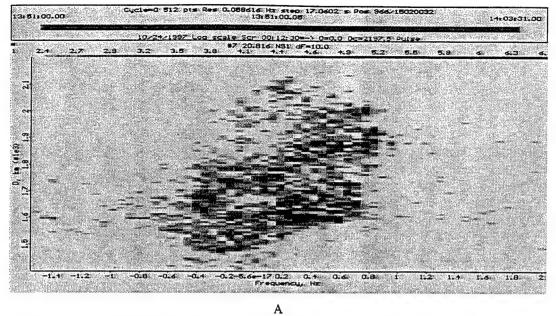
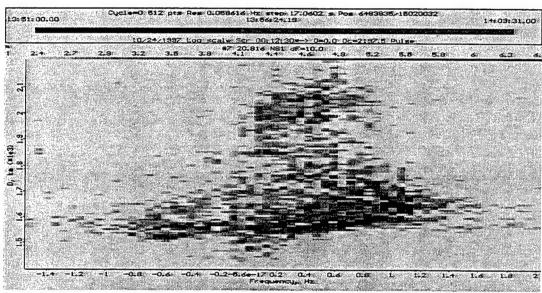


Fig. 9. Scattered intensity in the frequency-range coordinates for different phases of geomagnetic pulsations.





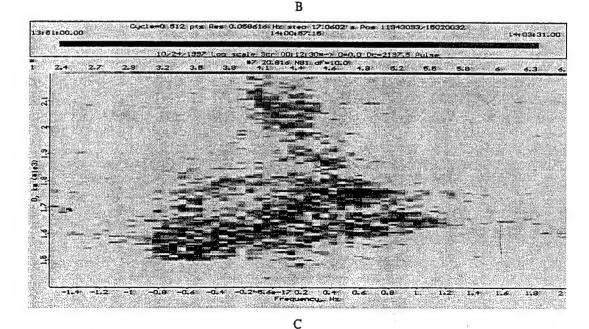
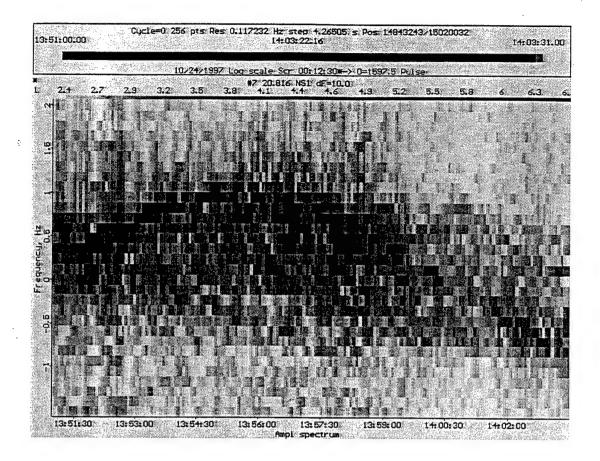


Fig. 10. Scattered intensity in the frequency-range coordinates for different time moments.

i danisi da



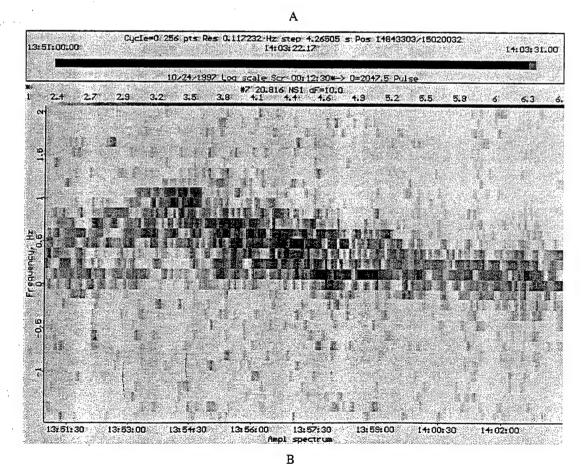


Fig. 11. Quasiperiodic variations in the Doppler frequency shift observed at different ranges.

Still another effect that had not been observed before was scattering of the diagnostic wave by a sporadic  $E_S$  layer. Fig. 12 shows a range-time map carrying a distinct signature at 300 to 350 km, along with the ground wave and a weak echo from the modified area. It should be emphasized that the condition of the ionosphere was characterized, through the entire period of observations, by considerable disturbance and frequent appearance of the sporadic  $E_S$  layer. Given the elevation angle of the reception beam (i.e. 20°), the height of scattering from  $E_S$  can be easily estimated ( $h = 300 \cdot \sin 20^\circ = 93$  km).

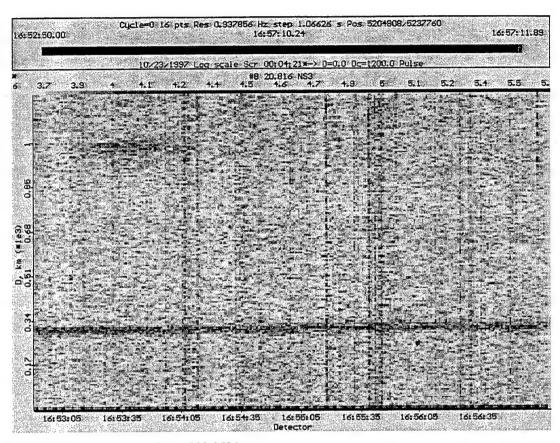


Fig. 12. Ionospheric scattering at 300-350 km.

A major task of the trial campaign was elaborating the technique and performing test measurements in the scanning mode of the multibeam reception pattern, with the aim of investigating the spatial structure of the scattering volume. Evidently, restoration of the 3D geometry is feasible with the use of pulsed diagnostic signals. The results of processing the data measured in one of the scanning sessions are given in Fig. 13. The azimuth angle of the scattering region (degrees) is along the abscissa and the relative range for true values of the elevation angle (18, 20 and 22 degrees) is along the vertical axis. The radar frequency is 20.816 kHz. In other words, Figures A through C can be regarded as horizontal-plane "cuts" of the investigated volume. The non-uniform spatial structure of the modified region is easily observable. It should be noted, however, that the pattern results from a three-minute scan taken on the assumption of stationarity of the spatial structure revealed by the scattering volume. This is a fairly strong assumption.

17

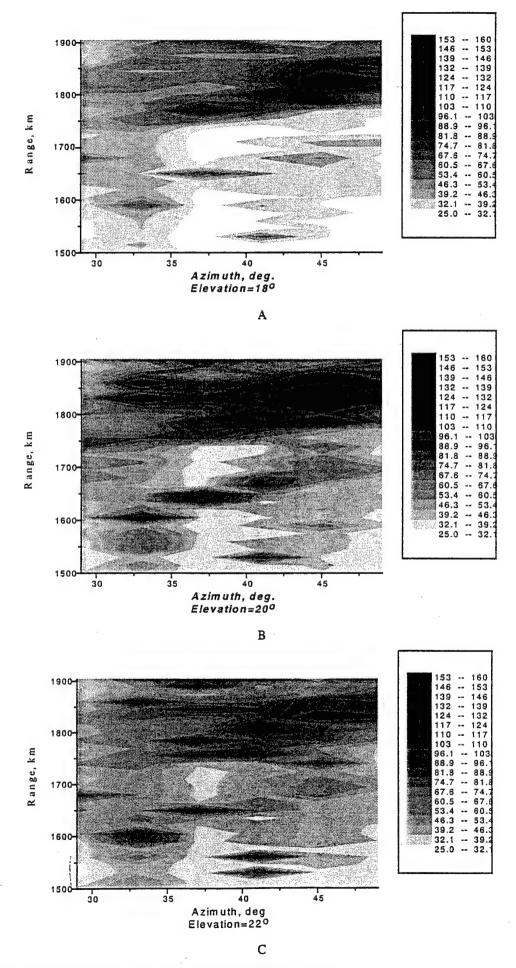


Fig. 13. Elevation-angle "cuts" of the modified ionospheric region.

The measurements of the pulsed radiation from Radio RWM actually have proven rather sensible too. Fig. 14 shows a range-time diagram demonstrating a signature of the scattered signal and its relaxation upon turn-off of the heating facility. In spite of the poor spatial resolution (3000 km for the 20 ms pulse), an estimate of the range to the scattering region can be obtained.

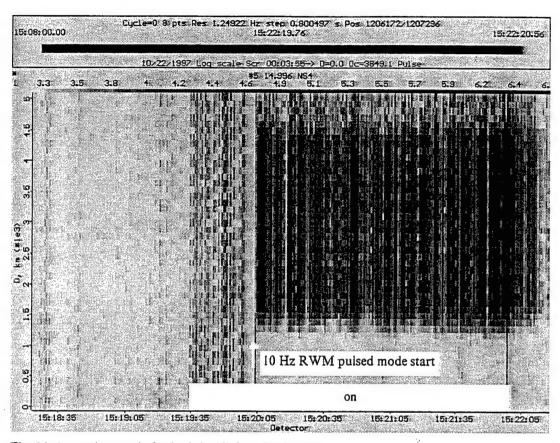


Fig. 14. A sample record of pulsed signals from Radio RWM.

Unfortunately, dual-frequency (19 and 21 MHz) measurements were only partially successful as echoes were observed at one of the sounding frequencies at a time. Apparently, this was due to the noticeable difference in the refraction, and hence in the conditions for aspect-sensitive scattering from field-aligned inhomogeneities.

#### 2.4. Geomagnetic Field Variations

Similar as in the 1995 campaign, variations in the geomagnetic field were recorded simultaneously with the radar observations of stimulated ionospheric turbulence. The magnetic measurements were carried out at the Astronomy Observatory of the University of Kharkov, close to the radar receive site. The experiment was aimed at investigating the effect of natural magnetohydrodynamic (MHD) waves that manifest themselves at the ground level as geomagnetic pulsations, upon parameters of the ionospheric inhomogeneities.

The variations in  $\hat{H}$  were recorded with an induction type magnetometer MM-II of the Space Radio Physics Laboratory of the University. The instrument has been designed by the Institute of Terrestrial Physics (Moscow, Russia) specially for registering geomagnetic pulsations over the range 0.001

to 2 Hz. It employs active induction type sensors with a differential frequency response, which permits compensating the effects of non-uniform spectral density of the natural field itself. Accordingly, the sensitivity threshold of the instrument is frequency dependent, making  $0.005 \gamma$  at 1 Hz and  $0.5 \gamma$  at 0.01 Hz. These parameters are greatly superior to such of the standard equipment of geomagnetic observatories, and enable recording pulsations of a few tenths of one gamma in amplitude. In addition, the magnetometer is equipped with a bank of analog band-pass filters for the traditional observatory treatment of the signals in narrow band channels of 0.2 to 2 Hz; 0.01 to 0.2 Hz and 0.00166 to 0.01 Hz. Of special interest for the present investigation were magnetic field variations with characteristic periods of a few tens of seconds (Pc3, Pc4 and Pi2 pulsations). Therefore, the data were filtered within the 0.01 to 0.2 Hz band. Then the data were digitized with the sampling frequency of 2 Hz and recorded on the hard disk of a PC486. The calibration curve (frequency response) of the «through» registration channel of magnetic variations is given in Fig. 15. The vertical axis represents the magnitude of the channel response (in terms of ADC counts) to a  $1 \gamma$  disturbance.

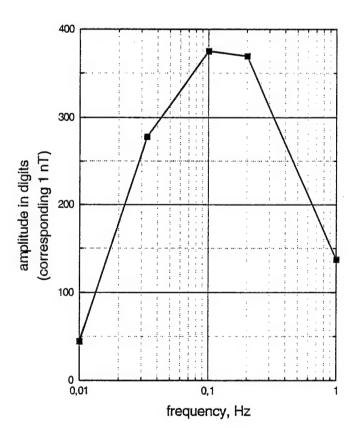


Fig. 15. Calibration curve for the magnetometer data.

The magnetic data were recorded October 17 through 31 in a practically continuous way, except the periods of planned interruptions of the power supply (2 to 4 hours per day, normally about noon, occasionally at early night). The records totally overlap the operating periods of the heating transmitter. The integrated duration of magnetic records in the 1997 campaign is 300 hr

(compared to 50 hr in 1995). In contrast to the 1995 measurements, two horizontal components of the magnetic field vector were measured, specifically the meridional,  $H_x$ , and the latitudinal,  $H_y$  (in 1995  $H_x$  was the only component measured). In principle, this may permit recovering the polarizational structure of the magnetic field variations. Fig. 16 (A and B) gives examples of daylong dynamic spectra of the magnetic field variations (horizontal  $\vec{H}$  components) recorded October 25, 1997. The spectra demonstrate an increasing activity of Pc3 pulsations (periods of 20-25 s) during day hours. This observation is in agreement with the general concept of such pulsations which are resonant Alfvenic vibrations of the geomagnetic lines of force, excited under the impact of solar wind on the day side of the magnetosphere [3]. Analysis of the finer spectral structures in both orthogonal components, carried out for the interval 10:00 to 17:00 (Fig. 17), has shown the variations of  $H_x$  to posses a distinct maximum near 0.04 Hz. The  $H_y$  component is characterized by a broader spectrum of variations, with a maximum at a higher frequency. In addition, a transient increase in the level of 0.03 Hz pulsations (period of 30 s) about 08:00 hours (local time) can be noted.

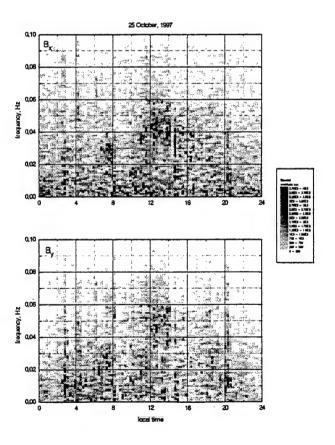


Fig. 16. Dynamic spectra of the magnetic field variations (horizontal  $\bar{H}$  components).

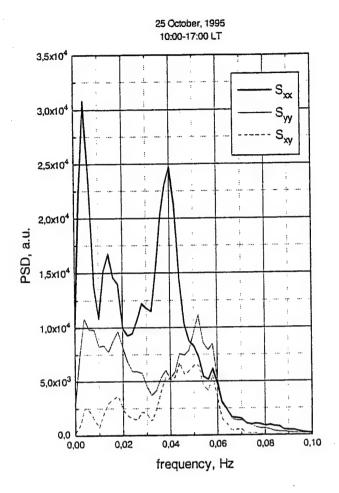


Fig. 17. Spectral structures of orthogonal geomagnetic field components.

Fig. 18A shows simultaneous records of Pc3 geomagnetic pulsations and the Doppler frequency shift,  $f_D$ , of the ionospherically scattered HF signals. The shift is proportional to the line-of-sight drift velocity of stimulated ionospheric inhomogeneities. As is easy to see, both sets of data demonstrate quasiperiodic variations with close values of the period,  $T \approx 30$  s. Using the calibration curve of Fig. 15, the variation amplitude in either horizontal H-component (about 100 ADC counts) can be estimated as 0.4 to 0.5 y. The power spectra of variations in the magnetic field and the Doppler velocity (Fig. 18B) show a fairly complex structure. Along with the maxima at their common frequency 0.033 Hz they produce extra peaks, specifically at 0.027 Hz for  $H_x$  and  $H_y$ , and 0.048 Hz for  $f_D$ . It should be remembered that the ground level and ionospheric data can be compared correctly if they relate to the same tube of magnétic lines. It is not so in our case as the McIlwain parameter for the tube passing through the Sura location is L=2.4, while the magnetic measurements near Kharkov were for L=2.0. In other words, the magnetic tubes might be different. The «horizontal» scale length of the magnetic pulsations is about 1000 km, which value is comparable with the separation between Kharkov and Sura. For these reasons the spectra of  $f_D$  and  $H_{xy}$  might be different.

To summarize, the magnetometric equipment that was available during the campaign enabled precision measurements of geomagnetic field variations. Combined with the radar meas-

urements of pulsation parameters at ionospheric altitudes, such data can serve as additional source of information on the properties of magnetohydrodynamic disturbances in the ionosphere.

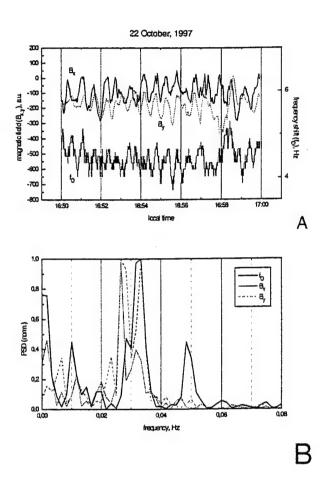


Fig. 18. Records of Pc3 geomagnetic pulsations and Doppler frequency shift variations (A) and their power spectra (B).

### Conclusion

The trial measuring campaign conducted with the use of the up-graded bistatic HF radar has demonstrated its ability to perform parallel dual-frequency sounding of stimulated ionospheric turbulence.

Compared with the prior experiments [1], the radiated power of the sounding pulses has been increased and the range of operating frequencies extended. Owing to the increased data processing rate it has proven possible to double the number of data channels to receive pulsed signals. Similarly, the magnetometric complex permits measuring two horizontal magnetic field components instead of one.

The minor technological drawbacks of the modified radar that were identified during the trial campaign have been removed.

Several new measurement techniques have been tested in the "heating" experiment. E.g., the reception pattern of the radar was scanned both in the elevation angle and azimuth; an extra diagnostic transmitter (frequency of 23.725 MHz) was operated at a new location near Novo-

cherkassk, Russia; the powerful "heating" emission from the Sura transmitter was monitored; the time-and-space structure of the modified ionospheric region was investigated for the vertically and obliquely incident "heating" radiation.

Part of the results obtained in the measuring campaign are given above in this Report, however much of the data require detailed processing and analysis.

The major result of the trial campaign is preparedness of the modified transmitter, receiver and data collection/data processing system to the main session of measurements due in the spring of 1998.

#### References

- Y.M. Yampolski, V.S. Beley, S.B. Kascheev, A.V. Koloskov, V.G. Somov, D.L. Hysell, B. Isham, and M.C. Kelley. Bistatic HF radar diagnostics induced field-aligned irregularities. JGR, Vol. 102, No A4, 1997, p. 7461 - 7467.
- 2. Frequency and Time Reference Signals: Official Bulletin B09 1991. Moscow, 1991, 39 p.
- Parkinson W.D. Introduction to geomagnetism. Scottish Academic Press, Edinburg and London, 1983.

to 2 Hz. It employs active induction type sensors with a differential frequency response, which permits compensating the effects of non-uniform spectral density of the natural field itself. Accordingly, the sensitivity threshold of the instrument is frequency dependent, making 0.005 γ at 1 Hz and 0.5 γ at 0.01 Hz. These parameters are greatly superior to such of the standard equipment of geomagnetic observatories, and enable recording pulsations of a few tenths of one gamma in amplitude. In addition, the magnetometer is equipped with a bank of analog band-pass filters for the traditional observatory treatment of the signals in narrow band channels of 0.2 to 2 Hz; 0.01 to 0.2 Hz and 0.00166 to 0.01 Hz. Of special interest for the present investigation were magnetic field variations with characteristic periods of a few tens of seconds (Pc3, Pc4 and Pi2 pulsations). Therefore, the data were filtered within the 0.01 to 0.2 Hz band. Then the data were digitized with the sampling frequency of 2 Hz and recorded on the hard disk of a PC486. The calibration curve (frequency response) of the «through» registration channel of magnetic variations is given in Fig. 15. The vertical axis represents the magnitude of the channel response (in terms of ADC counts) to a 1 γ disturbance.

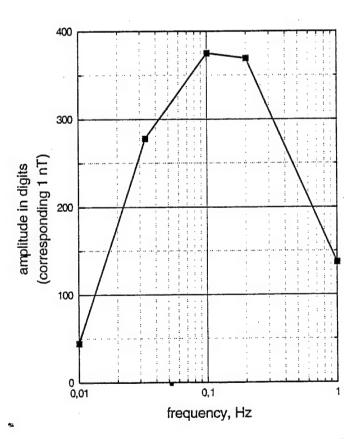


Fig. 15. Calibration curve for the magnetometer data.

The magnetic data were recorded October 17 through 31 in a practically continuous way, except the periods of planned interruptions of the power supply (2 to 4 hours per day, normally about noon, occasionally at early night). The records totally overlap the operating periods of the heating transmitter. The integrated duration of magnetic records in the 1997 campaign is 300 hr

(compared to 50 hr in 1995). In contrast to the 1995 measurements, two horizontal components of the magnetic field vector were measured, specifically the meridional,  $H_x$ , and the latitudinal,  $H_y$  (in 1995  $H_x$  was the only component measured). In principle, this may permit recovering the polarizational structure of the magnetic field variations. Fig. 16 (A and B) gives examples of daylong dynamic spectra of the magnetic field variations (horizontal  $\vec{H}$  components) recorded October 25, 1997. The spectra demonstrate an increasing activity of Pc3 pulsations (periods of 20-25 s) during day hours. This observation is in agreement with the general concept of such pulsations which are resonant Alfvenic vibrations of the geomagnetic lines of force, excited under the impact of solar wind on the day side of the magnetosphere [3]. Analysis of the finer spectral structures in both orthogonal components, carried out for the interval 10:00 to 17:00 (Fig. 17), has shown the variations of  $H_x$  to posses a distinct maximum near 0.04 Hz. The  $H_y$  component is characterized

by a broader spectrum of variations, with a maximum at a higher frequency. In addition, a transient increase in the level of 0.03 Hz pulsations (period of 30 s) about 08:00 hours (local time) can

be noted.

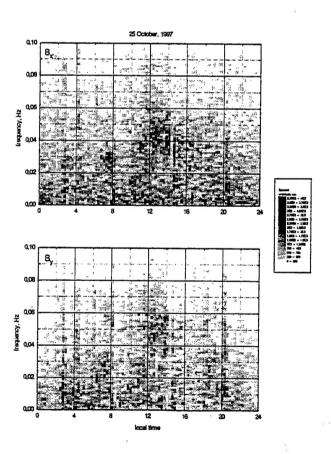


Fig. 16. Dynamic spectra of the magnetic field variations (horizontal  $\vec{H}$  components).

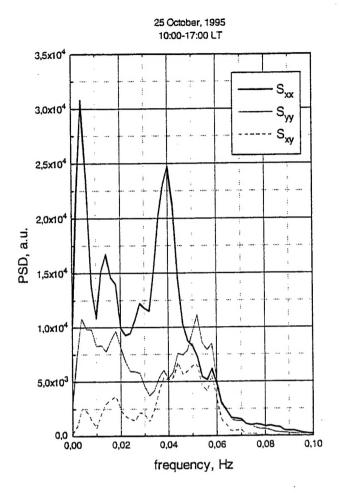


Fig. 17. Spectral structures of orthogonal geomagnetic field components.

Fig. 18A shows simultaneous records of Pc3 geomagnetic pulsations and the Doppler frequency shift,  $f_D$ , of the ionospherically scattered HF signals. The shift is proportional to the line-of-sight drift velocity of stimulated ionospheric inhomogeneities. As is easy to see, both sets of data demonstrate quasiperiodic variations with close values of the period,  $T \approx 30$  s. Using the calibration curve of Fig. 15, the variation amplitude in either horizontal H-component (about 100 ADC counts) can be estimated as  $0.4 \text{ to } 0.5 \text{ }\gamma$ . The power spectra of variations in the magnetic field and the Doppler velocity (Fig. 18B) show a fairly complex structure. Along with the maxima at their common frequency 0.033 Hz they produce extra peaks, specifically at 0.027 Hz for  $H_x$  and  $H_y$ , and 0.048 Hz for  $f_D$ . It should be remembered that the ground level and ionospheric data can be compared correctly if they relate to the same tube of magnetic lines. It is not so in our case as the McIlwain parameter for the tube passing through the Sura location is L=2.4, while the magnetic measurements near Kharkov were for L=2.0. In other words, the magnetic tubes might be different. The «horizontal» scale length of the magnetic pulsations is about 1000 km, which value is comparable with the separation between Kharkov and Sura. For these reasons the spectra of  $f_D$  and  $H_{x,y}$  might be different.

To summarize, the magnetometric equipment that was available during the campaign enabled precision measurements of geomagnetic field variations. Combined with the radar meas-

urements of pulsation parameters at ionospheric altitudes, such data can serve as additional source of information on the properties of magnetohydrodynamic disturbances in the ionosphere.

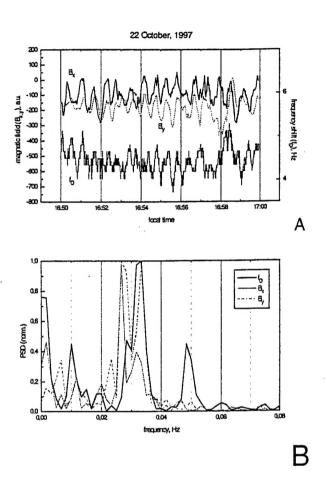


Fig. 18. Records of Pc3 geomagnetic pulsations and Doppler frequency shift variations (A) and their power spectra (B).

#### Conclusion

The trial measuring campaign conducted with the use of the up-graded bistatic HF radar has demonstrated its ability to perform parallel dual-frequency sounding of stimulated ionospheric turbulence.

Compared with the prior experiments [1], the radiated power of the sounding pulses has been increased and the range of operating frequencies extended. Owing to the increased data processing rate it has proven possible to double the number of data channels to receive pulsed signals. Similarly, the magnetometric complex permits measuring two horizontal magnetic field components instead of one.

The minor technological drawbacks of the modified radar that were identified during the trial campaign have been removed.

Several new measurement techniques have been tested in the "heating" experiment. E.g., the reception pattern of the radar was scanned both in the elevation angle and azimuth; an extra diagnostic transmitter (frequency of 23.725 MHz) was operated at a new location near Novo-

cherkassk, Russia; the powerful "heating" emission from the Sura transmitter was monitored; the time-and-space structure of the modified ionospheric region was investigated for the vertically and obliquely incident "heating" radiation.

Part of the results obtained in the measuring campaign are given above in this Report, however much of the data require detailed processing and analysis.

The major result of the trial campaign is preparedness of the modified transmitter, receiver and data collection/data processing system to the main session of measurements due in the spring of 1998.

#### References

- Y.M. Yampolski, V.S. Beley, S.B. Kascheev, A.V. Koloskov, V.G. Somov, D.L. Hysell, B. Isham, and M.C. Kelley. Bistatic HF radar diagnostics induced field-aligned irregularities. JGR, Vol. 102, No A4, 1997, p. 7461 - 7467.
- 2. Frequency and Time Reference Signals: Official Bulletin B09 1991. Moscow, 1991, 39 p.
- Parkinson W.D. Introduction to geomagnetism. Scottish Academic Press, Edinburg and London, 1983.